Electronic Materials Letters, Vol. 5, No. 2 (2009), pp. 73-76
DOI: 10.3365/eml.2009.06.073

Origin of Low Photocatalytic Activity of Rutile TiO_2

Hyun Suk Jung[1] and Hyungtak Kim[2,*]

[1]School of Advanced Materials Engineering, Kookmin University,
Jeongneung-dong, Seongbuk-gu, Seoul 136-702, Korea
[2]School of Electronic & Electrical Engineering, Hongik University,
72-1 Sangsu-dong, Mapo-gu, Seoul 121-791, Korea

Rutile TiO_2 nanoparticles were synthesized using the colloidal sol-gel process and their photocatalytic properties were characterized in comparison with anatase TiO_2 nanoparticles. The synthesized rutile nanoparticles were found to possess higher surfaces area than the anatase nanoparticles and to exhibit lower photocatalytic activities, demonstrating that rutile TiO_2 has intrinsically low photocatalytic properties. The photoluminescence (PL) study suggested that the inferior photocatalytic activity of rutile nanoparticles is correlated with the intrinsic recombination of photogenerated electron-hole pairs.

Keywords: Photocatalyst, Nanoparticle, Rutile, Anatase, Charge recombination

1. INTRODUCTION

The unique characteristics of TiO_2 such as its effective extraction of photogenerated carriers and photocatalytic activity under UV irradiation have made it very attractive for potential applications in solar energy conversion or the photocatalytic decomposition of pollutants.[1,2] TiO_2 has three polymorphic phases: anatase, brookite and rutile phases. The anatase and brookite TiO_2 are thermodynamically metastable phases and the rutile is a stable phase.[1,3] Many studies have focused on the anatase TiO_2 because of its superior photocatalytic properties in comparison with rutile TiO_2.[2-5] Usually, rutile TiO_2 has been synthesized by thermal calcinations at a high temperature (400°C to 1000°C), which results in undesirable aggregation and sintering and a consequent decrease in specific surface area [6,7]. Thus far, it has not been clearly understood whether the low photoactivity of rutile TiO_2 can be attributed to the low surface area originating from the high-temperature calcinations or to an intrinsic property.

In the present study, rutile nanoparticles with a high surface area were successfully synthesized by a sol-gel colloidal process. A systematic study on the photocatalytic activities of rutile TiO_2 nanoparticles was performed in comparison with those of anatase nanoparticles of comparable surface area.

2. EXPERIMENTAL PROCEDURE

2.1. Preparation of TiO_2 colloidal sols and powders

Titanium tetraisopropoxide (TTIP, $Ti(OiPr)_4$, 97%, Aldrich Chemicals Co.) was hydrolyzed with excess water ($[H_2O]/[Ti] = 50$) at 30°C and stirred for 24 h at the same temperature. Nitric acid ($[H+]/[Ti] = 1.25$) was added to the aforementioned solution, followed by further aging for 1 week. The resultant TiO_2 colloidal sol is designated as R0. The anatase particles were obtained using a similar process, which is presented elsewhere.[8]

The obtained R0 sol was washed with deionized water 12 times using a centrifuge. At the final washing, the pH was 6.4. The washed TiO_2 sol was frozen instantaneously with liquid nitrogen. The frozen sample was dried in a freeze-drying machine (50°C and 103 Torr) for 24 h in order to prevent the TiO_2 particles from agglomerating. A detailed explanation of the preparation method for the anatase particles was presented in the previous work.

2.2. Fabrication of TiO_2 films

To fabricate the TiO_2 films, alcohol-based colloidal sols were prepared using a ball-milling system, which contained 3 g of TiO_2 powders (rutile and anatase powders) and 40 ml of ethanol. The rutile and anatase films were fabricated by a spin-coating method using the prepared TiO_2 colloidal sols. The obtained TiO_2 films were annealed at the scheduled temperatures (300°C, 450°C, and 600°C) and then designated as R0 (as deposited), R300, R450 and R600, respectively. The anatase film, annealed at 600°C, was denoted as A600. The thickness of the prepared thin films was approximately 400 nm-600 nm, estimated using scanning electron microscopy.

2.3. Characterization

The crystal structure of the TiO_2 films was analyzed with

*Corresponding author: hkim@wow.hongik.ac.kr

the aid of X-ray diffraction (XRD). Data collection was performed in the 2θ range of 20° to 33° using Cu Ká radiation (Model: M18XHF, Macscience Instruments, Japan). The specific surface area of the powder annealed under the same conditions as the thin film was measured using a surface analyzer (ASAP2010, Micromeritics Instrument Group, USA). Transmission electron microscopy (TEM, JEOL JEM 200-CX) was used to investigate the morphologies and crystal structure of the powders. Photoluminescence (PL) measurements were performed using an Nd-YAG laser at room temperature.

The photoactivity of the fabricated TiO_2 films was measured by casting the TiO_2 films with thin films of stearic acid [$CH_3(CH_2)_{16}COOH$] and measuring at a defined irradiance the rate of decrease in the integrated absorbance of the ensemble of the C-H stretching vibrations between 2800 cm^{-1} and 3000 cm^{-1}, using FTIR spectroscopy (Bomen DA8-12). A 10 W lamp (SANYO) was used as a UV light source.

3. RESULTS AND DISCUSSION

As shown in Fig. 1, only rutile (110) peak was found, which indicates that the TiO_2 film is composed of pure rutile phase. Given that the full width at half maximum (FWHM) of the rutile (110) peak reduces as a function of the annealing temperature, the size of rutile nanoparticles in the films increases with the annealing temperature. In the A600 film, only anatase (101) peak was found and no rutile phase was observed. The FWHM rutile (110) peak from the R0 and R300 samples is wider than that of the A600 sample, which shows that the crystallite size of the R0 and R300 rutile samples is smaller than that of the anatase A600 sample.

The specific surface areas of the TiO_2 nanoparticles, which were annealed under the same conditions as the thin films, were measured. The BET surface areas for each powder are plotted in Fig. 2. The BET surface area of the R0 powder was 137.68 m^2/g, which was significantly decreased to 23.11 m^2/g after annealing at 600°C (R600). Given the BET surface of anatase (A600), 20.87 m^2/g, the overall BET surface areas for rutile nanoparticles are larger than that of anatase. These results demonstrate that the anatase nanoparticles annealed at 600°C possess either a larger crystallite size than do rutile nanoparticles or a highly agglomerated structure.

TEM micrographs of each powder, obtained by scratching the mother films, are presented in Fig. 3. The average crystallite size (length and width) estimated from TEM micrographs is plotted in Fig. 4. The rutile nanoparticles (R0, R450, and R600) exhibit 1-dimensional nanostructure (needle or rod). The average crystallite size was approximately 7

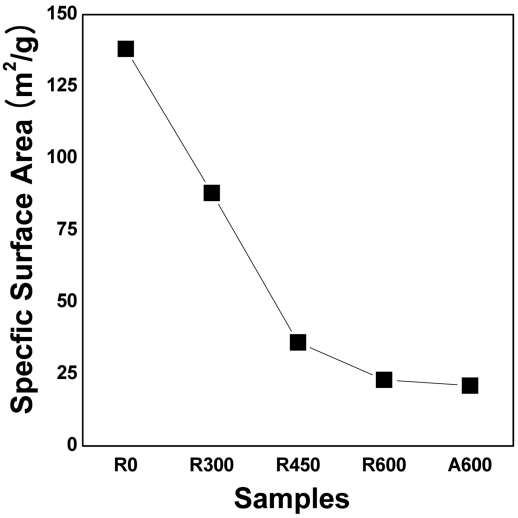

Fig. 2. Specific surface areas of rutile (R0, R300, R450, and R600) and anatase nanoparticles (A600).

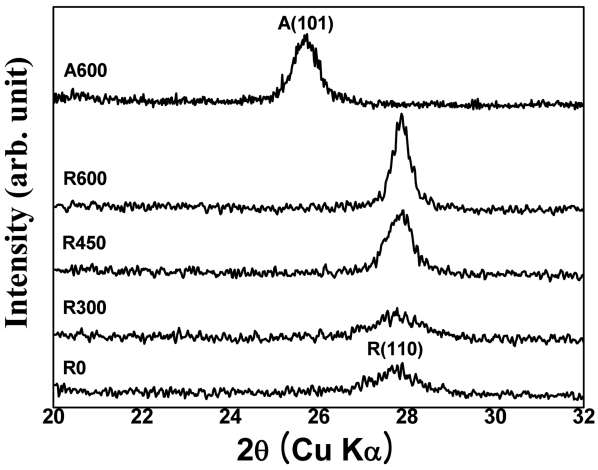

Fig. 1. XRD reflections of TiO_2 anatase (A600) and rutile (R0, R300, R450, and R600) films.

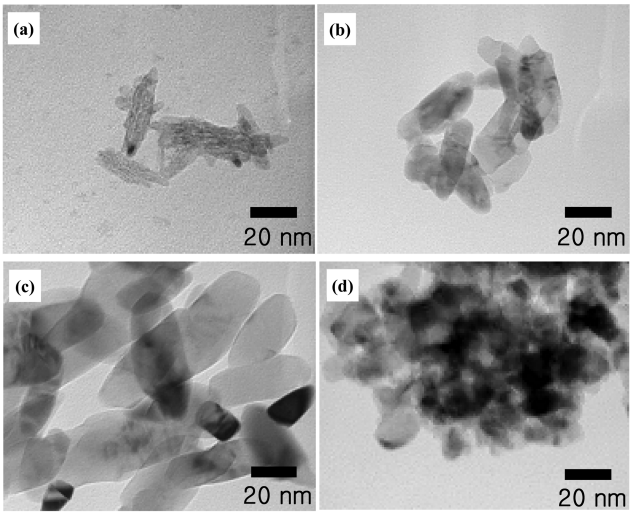

Fig. 3. TEM micrographs of (a) R0, (b) R450, (c) R600, and (d) A600 powders. All samples were obtained by scratching the TiO_2 films.

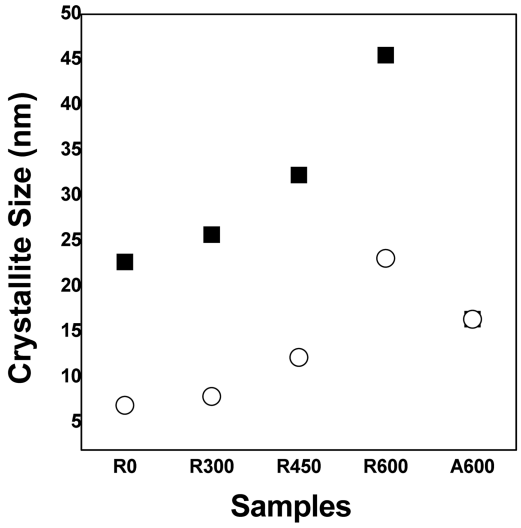

Fig. 4. Change in the crystallite size of rutile and anatase nanoparticles (■ : length and ○ : width).

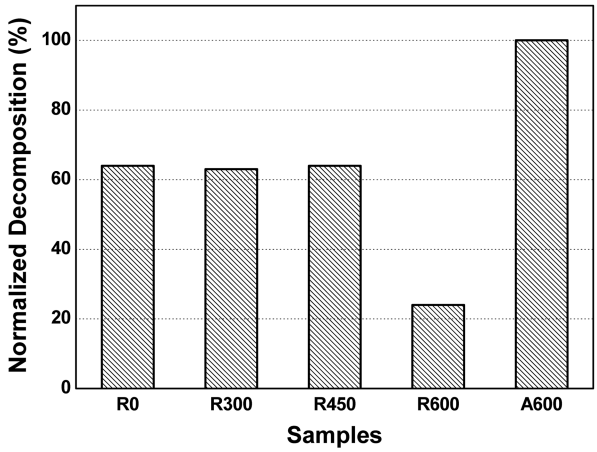

Fig. 5. Photocatalytic properties of rutile (R0, R300, R450, and R600) and anatase nanoparticles (A600).

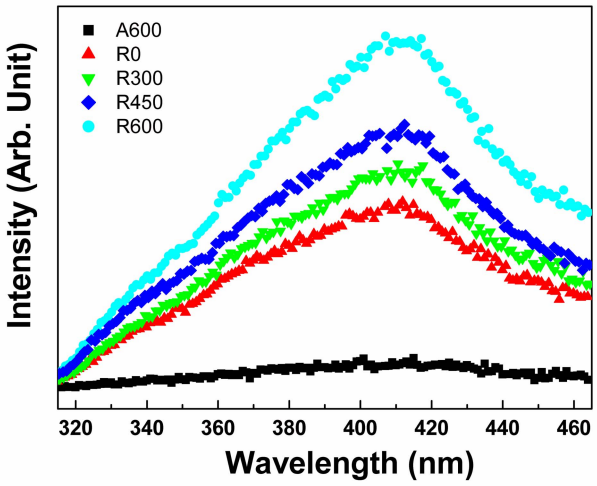

Fig. 6. PL spectra for rutile and anatase films (■ : A600, ▲ : R0, ▼ : R300, ◆ : R450, and ● : R600).

nm × 23 nm (width × length) for R0, which increased to 23 nm × 45 nm after annealing at 600°C. The A600 anatase crystallites are rather 0-dimensional and the crystallite size is approximately 16 nm in diameter. The porous structure of R0 particles (Fig. 3(a)) is responsible for the large BET value. Also, the change into dense structure as a function of annealing temperature accounts for the decrease in the BET values of rutile nanoparticles. As shown in Fig. 3(d), the low BET value is associated with the severely agglomerated structure.

Figure 5 shows the photocatalytic properties of the rutile (R0, R300, R450, and R600) and anatase films (A600), clearly demonstrating that the photocatalytic activities of all of the rutile films are lower than that of the anatase film. The relative amount of decomposed stearic acid for the R0 film is approximately 64% and is significantly decreased with the annealing process. In contrast, the anatase film (A600) completely removes the stearic film, which indicates that the photocatalytic activity for the anatase film is much superior to that for the rutile film.

Rutile TiO_2 has been reported to possess lower photocatalytic activity than anatase TiO_2.[2-5] Usually, rutile particles are obtained from high-temperature calcination, which results in significant growth of particles.[6,7] The origin of the lower photocatalytic activity of rutile TiO_2 is elusive; i.e., the dominant contribution between the intrinsic effect and low surface area has not yet been clearly elucidated. In the present study, rutile nanoparticles with a high surface area were successfully prepared using a low temperature colloidal process and exhibited lower photocatalytic activities than anatase nanoparticles with a low surface area, demonstrating that the low photocatalytic activity of rutile nanoparticles is not correlated with the surface area.

Figure 6 shows the photoluminescence (PL) spectra of rutile (R0, R300, R450, and R600) and anatase (A600) thin films, respectively. The rutile films show an emission peak at approximately 410 nm. However, no emission spectrum is found in the anatase film. The intensity of the PL peak for the rutile films increases with the annealing temperature. These results indicate that the recombination of photogenerated electrons and holes takes place in rutile films[9,10] and that the degree of recombination increases with the annealing temperature. In this regard, the low photocatalytic activities of rutile films would be ascribed to the radiative recombination process of photogenerated electrons and holes. In addition, the significantly deteriorated photocatalytic activity for R600 film would be correlated with the recombination process as well as with the decreased surface area. Yu *et al.*[10] reported that fluorine-doped anatase films with low intensity PL spectra showed a high photocatalytic activity.

Although the origin of the severe radiative recombination of rutile films is not clear, it might be attributed to the difference in the effective mass. The effective mass for anatase TiO_2 has been reported to be 1.9. In case of rutile TiO_2, the effective electron mass is much heavier than those for anatase, which range from 3 to 30.[11,12] The heavier effective electron mass is responsible for the slow mobility of rutile TiO_2, which is 40 times lower than that of anatase TiO_2. Therefore, the sluggish electron mobility of rutile TiO_2 may induce the severe recombination process, which is correlated with the low photocatalytic activity.

4. CONCLUSIONS

In summary, the photocatalytic properties of rutile nanoparticles were systematically investigated in comparison with anatase nanoparticles. Although the rutile nanoparticles possess higher surface area than do the anatase nanoparticles, the photocatalytic properties of the rutile nanoparticles were much lower than those of the anatase nanoparticles. The photoluminescence study demonstrates that the origin of low photocatalytic activity for rutile TiO_2 is associated with the intrinsic radiative recombination of photogenerated electrons and holes.

ACKNOWLEDGMENT

This work was supported by a grant from the Korea Science and Engineering Foundation (KOSEF) of the Korean government (MEST) (R11-2005-048-00000-0, ERC, CMPS and R01-2008-000-20581-0). This work was also supported by the Seoul R&BD Program (CR070027C092852) and the 2009 research program of Kookmin University in Korea.

REFERENCES

1. M. W. Park and K. Y. Chun, *Electron Mater. Lett.* ***5***, 7 (2009).
2. S. H. Yoo, *Electron Mater. Lett.* ***2***, 195 (2006).
3. S. Won, S. Go, K. Lee, and J. Lee, *Electron. Mater. Lett.* ***4***, 29 (2008).
4. H. Tada, and H. Honda, *J. Electrochem. Soc.* ***142***, 3438 (1995).
5. K. Kato, A. Tsuzuki, H. Taoda, Y. Torii, T. Kato, and Y. *J.* Butsugan, *Mater. Sci.* ***29***, 5911 (1994).
6. R. D. Shannon and J. A. Pask, *J. Am. Ceram. Soc.* ***48***, 391 (1965).
7. K.-N. P. Kumar, J. Kumar, and K. *J.* Keizer, *Am. Ceram. Soc.* **77**, 1396 (1994).
8. H. S. Jung, H. Shin, J. R. Kim, J. Y. Kim, K. S. Hong, and J. K. Lee, *Langmuir* **20**, 11732 (2004).
9. Y. C. Lee, Y. P. Hong, H. Y. Lee, H. Kim, Y. J. Jung, K. H. Ko, H. S. Jung, and K. S. Hong, *J. Colloid Interf. Sci.* **267**, 127 (2003).
10. J. C. Yu, J. Yu, W. Ho, J. Zitao, and L. Zhang, *Chem. Mater.* **14**, 3808 (2002).
11. M. Voinov and J. Augustynski, *Heterogeneous Photocatalysis*, 1, (ed., M. Schiavello) John Wiley and Sons, New York (1997).
12. M. Kaneko and I. Okura, *Photocatalysis*, Springer, New York (2002).